Resonances of Modified Bowtie Nanoparticles with Higher Field Enhancements

Karlo Q. da Costa, and Victor Dmitriev

Abstract— **In this paper, we present an analysis of the resonant behavior of modified bowtie nanoparticles with polynomial sides. The method of moments is used to solve numerically the scattering problem. With this model, we investigate the variation of the spectral response and near field distribution in function of the length and polynomial order of the nanoparticles. The results show that these particles possess smaller number of resonances in the analyzed wavelength range and their resonant wavelength, near field enhancement and confinement are higher than those of the conventional bowtie particle with linear sides.**

Index Terms—**Surface plasmons, subwavelength structures, bowtie metal nanoparticles, spectral response.**

I. Introduction

THE electromagnetic scattering of metals in optical frequency region possesses special characteristics. At these frequencies, there are electron oscillations in the metal called plasmons with distinct resonant frequencies, which produce strongly enhanced near fields at the metal surface. This effect can be analyzed using Lorentz-Drude model of the complex dielectric constant. The science of the electromagnetic optical response of metal nanostructures is known as plasmonics or nanoplasmonics [1].

One of the possible applications of plasmonics is design of nanoantennas [2-8] which are metal nanostructures used to confine and enhance optical electromagnetic fields. An optical monopole antenna is investigated in [3]. In [4], Bowtie optical antennas are analyzed. Dipoles nanoantennas are presented in [5], and sphere nanoantennas are discussed in [6-7]. Bowtie nanoantennas with different length, bow angles, thickness, gap distance, and radius of curvature of the apex are studied in [8]. Examples of applications of these antennas are ultra-high-density data storage, super-resolution microscopy, integrated nano-optical devices and surface-enhanced Raman scattering [1]. Most of these antennas are composed of coupled metal nanoparticles. To understand the electromagnetic behavior of these nanoantennas is important to investigate the resonances and field distributions of individual particles. Some common metal nanoparticles have been analyzed, e.g. spheres [7], circular disk [9], and triangular disk [10].

K. Q. da Costa, and V. Dmitriev are with the Department of Electrical Engineering, Federal University of Para, Av. Augusto Corrêa, N1, CEP 66075-900, Belém-PA, Brazil, (e-mail: karlo@ufpa.br).

In the conventional triangular bowtie antennas, the sides are straight lines. In this paper, we present a theoretical analysis of modified bowtie nanoparticles with polynomial sides. We analyze the optical response of the proposed nanoparticles and the dependence of the optical response on the length and polynomial order. Near field distributions are also investigated. We apply the method of moments (MoM) [11] to calculate the optical scattering of these particles illuminated by a plane wave. The Lorentz-Drude theory with one interband term is used to model the complex permittivity of the gold.

We show that these particles have smaller number of resonances in the analyzed wavelength range and higher resonant wavelength, near field enhancement and confinement in comparison with that of the conventional bowtie particle. The next sections present the mathematical modeling of the scattering problem, numerical results, and conclusions.

II. Theory

The geometries of the modified bowtie nanoparticles are shown in Fig. 1. We investigate four particles made of gold (Au) with different values of the parameter α=(1,2,3,4) where α is the polynomial order of the side variation. The polynomial function used to model the curvature of the sides is $x=(y/k_1)^{\alpha}$, where $k_1=L/2h^{1/\alpha}$, $h=0.5L(3)^{0.5}$, L is the side length of the conventional bowtie triangle. The conventional bowtie particle where the side variation is linear corresponds to the case α=1. These particles are centered in the origin of the coordinate system with one tip oriented along the x axis. The thickness of the antennas (which is not shown) is w. With these parameters, the tip on the x axis is positioned at the point ($0.5h$; 0; 0). For higher values of α, the tips are more acute.

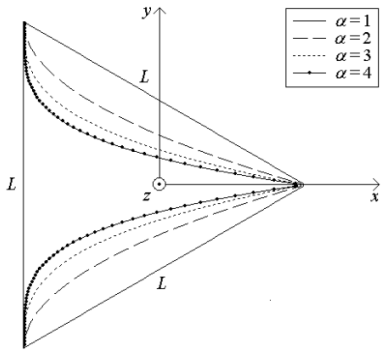

Fig. 1. Geometry of the Bowtie nanoparticles with polynomial sides.

The particles shown in Fig. 1 are illuminated by an Ex-polarized, z-directed plane wave. The numerical analysis of these scattering problems is fulfilled by our MoM code based on the model proposed in [11], where the equivalent polarization current inside the volume of the particles is determined by solving the tensor integral equation for the electric field. In this model, the volume of a particle is divided in N small cubic subvolumes, where the total electric field is approximately constant. With this approximation, the integral equation is transformed into a linear system with N_t=3N equations because there are three electric field components in each subvolume.

The Lorentz-Drude model with one interband term was used to model the complex permittivity ε=$\varepsilon_0\varepsilon_r$ of the Au particles, where ε_r is defined

$$\varepsilon_r = 1 - \frac{\omega_{p1}^2}{\omega^2 - j\Gamma\omega} + \frac{\omega_{p2}^2}{\omega_0^2 - \omega^2 + j\gamma\omega} + \varepsilon_\infty \qquad (1)$$

and the parameters of this equation are: ε_∞=6, ω_{p1}=13.8×1015s^{-1}, Γ=1.075×1014s^{-1}, ω_0=2$\pi c/\lambda_0$, λ_0=450nm, ω_{p2}=45×1014s^{-1}, and γ=9×1014s^{-1} [1]. This model is a good approximation in the range of wavelengths from 500 nm to 1800 nm. In this frequency range we fulfill our analysis.

III. Numerical Results

Based on theory presented previous section, four codes were developed in Fortran and Matlab. The discretization used in the bowtie nanoparticles with α=(1,2,3,4) are N_t=4380, 5310, 4410, and 5328, respectively. With these discretizations we obtained a good convergence of the results. For each nanoparticle, eight simulations were did with different values of length L, these values are L=50; 100; 150; 200; 250; 300; 350; and 400 (all in nanometers). The thickness w (in namometers) of the particles with L=50nm are 8.0; 8.3; 7.8; and 8.5 for the particles α=(1,2,3,4) respectively. The thickness of the others particles are proportional to these values, i.e. the particles with higher L possess higher thickness. The next sections present the obtained numerical results.

A. Spectral Responses

Figs. 2-5 present the spectral response of the field near the particles. The parameter shown in these figures is the field enhancement, which is defined by $(E/E_0)^2$, where E is the total electric field (incident and scattered) near the particle, and E_0 is the amplitude of the incident plane wave. In all these results, the field enhancement is calculated at 10nm far from the tip's particles along the x axis, i.e. at the point (0.5h+10nm; 0; 0).

We observe in these figures some characteristic resonances, which are numbered with 1 to 8, where the respective resonant wavelengths are λ_1 to λ_8. Some of these resonances for determined values of L are very weak, for example in Fig. 2 the resonance λ_1 is only significant for L=50 and 100nm, and it is practically null for other values of L. These very weak resonances are not shown in these figures.

The number of resonances varies with α, for α=(1,2,3,4) we have 8 (Fig. 2); 6 (Fig. 3); 6 (Fig. 4); and 2 (Fig. 5) resonances respectively, so for larger values of α smaller is the number of resonances. In general, these resonances are shifted to the right

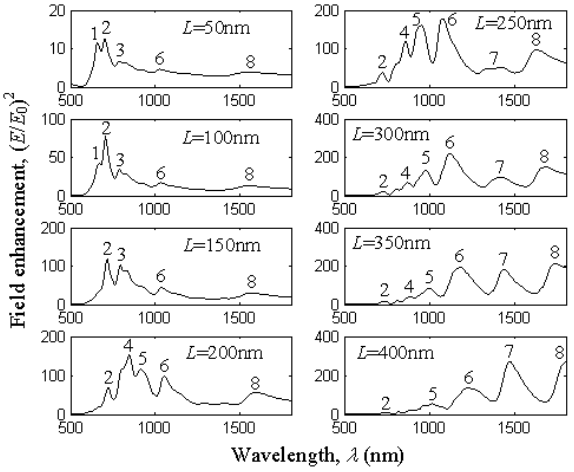

Fig. 2. Spectral response of field enhancement of the nanoparticles with α=1.

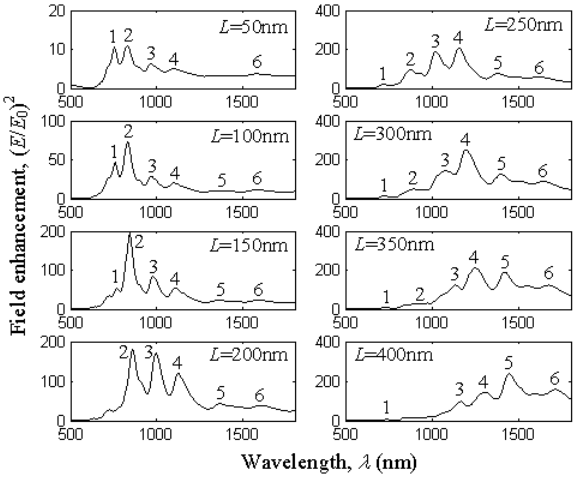

Fig. 3. Spectral response of field enhancement of the nanoparticles with α=2.

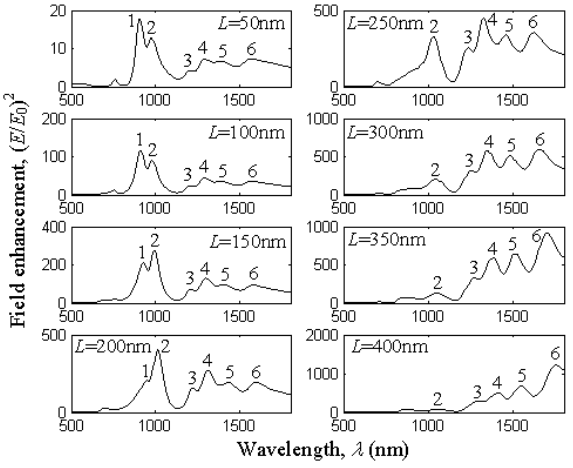

Fig. 4. Spectral response of field enhancement of the nanoparticles with α=3.

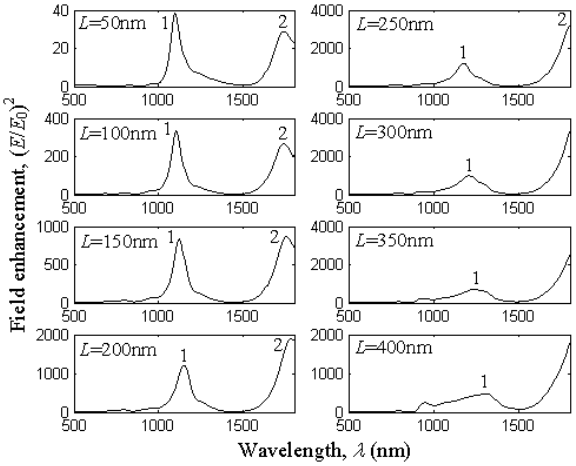

Fig. 5. Spectral response of field enhancement of the nanoparticles with α=4.

for larger lengths L and polynomial order α. However, the sensitivity of this variation with α is higher than with L. In all the cases shown in Figs. 2-5, we observe an approximately linear increasing of the resonances λ_1-λ_8 for larger values of L. This variation is presented in Figs. 6-9, where we note the increasing of the resonances with α, for example, for L=50nm, λ_1=660; 754; 903; and 1096 for α=(1,2,3,4) respectively.

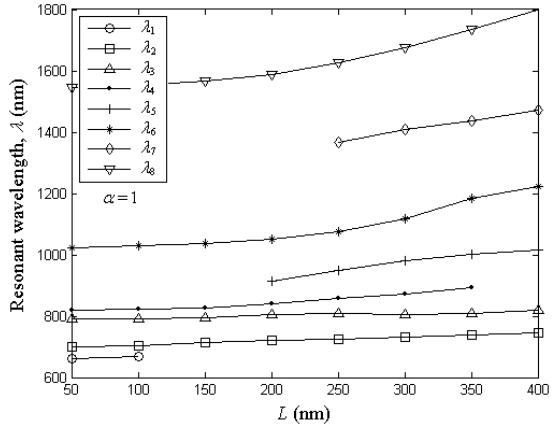

Fig. 6. Variation of λ_1-λ_8 versus L for the nanoparticles with α=1.

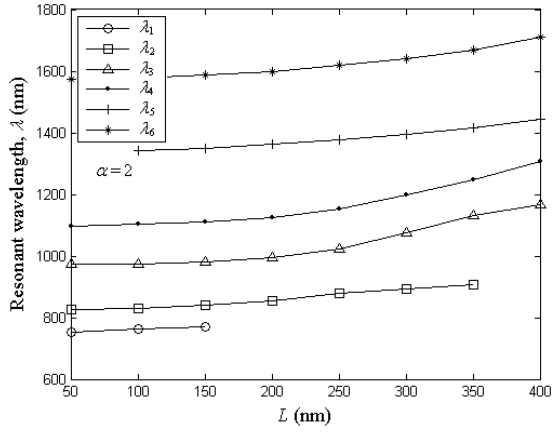

Fig. 7. Variation of λ_1-λ_6 versus L for the nanoparticles with α=2.

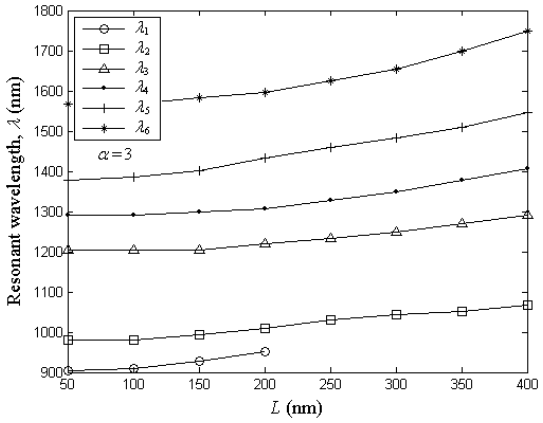

Fig. 8. Variation of λ_1-λ_8 versus L for the nanoparticles with α=3.

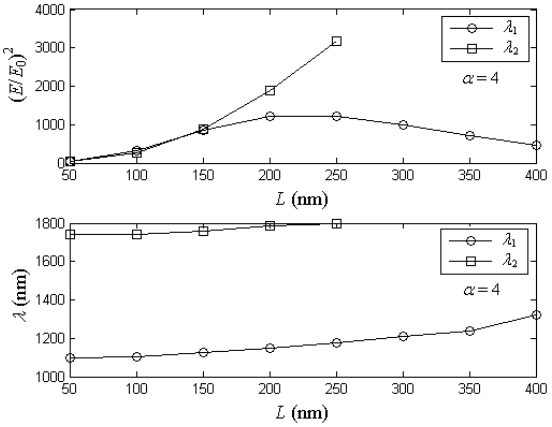

Fig. 9. Variation of $(E/E_0)^2$ and λ_1-λ_2 versus L for the nanoparticles with α=4.

With respect to the intensity of the resonances shown in Figs. 2-5, we observe that the field enhancement of each resonant is gradually increased and decreased with the variation of L, so that when one resonance is decreased, the next right resonance is increased. This behavior can be observed for example in the resonances λ_2 and λ_3 in Fig. 3, where for lower L (L=50; 100; 150; and 200nm), the field enhancement of λ_2 is higher than λ_3, and for L=250; 300; 350; and 400nm the field enhancement of λ_3 is higher than λ_2. This effect occurs progressively for all resonances.

There is a given L where the maximum value of $(E/E_0)^2$ for each resonance is achieved. Figs. 9-12 show this variation of the field enhancement at resonances λ_1-λ_8 versus L for the nanoparticles with α=(4,1,2,3), respectively. We note from these figures that the field enhancements is increased for larger values of α, i.e. the modified bowtie nanoparticles with polynomial sides possess higher field enhancements than the conventional bowtie particle with linear sides.

B. Near Field Distributions

Figs. 13-16 present the spatial distributions of the fields near the particles with α=(1,2,3,4), respectively. The results show the magnitude of the total field (E/E_0), and the components x (E_x/E_0), y (E_y/E_0), and z (E_z/E_0) at the plane z=9nm (−50nm<x,y<50nm). This plane is approximately 5nm above the particle's surface, because the thickness of them are

variable, i.e. w=8.0; 8.3; 7.8; and 8.5 (nm) for the particles with α=(1,2,3,4) respectively. In these figures, the size is L=50nm, and wavelengths are λ_2=703nm (Fig. 13), λ_2=827nm (Fig. 14), λ_1=907nm (Fig. 15), and λ_1=1096nm (Fig. 16).

We observe from these results that the modified bowtie nanoparticles with higher values of α (Figs. 14-16) possess the total field near the right tips more confined than that of the conventional one (Fig. 13). This shows that the modified bowtie nanoparticles with polynomial sides have a larger field confinement than the conventional triangular ones.

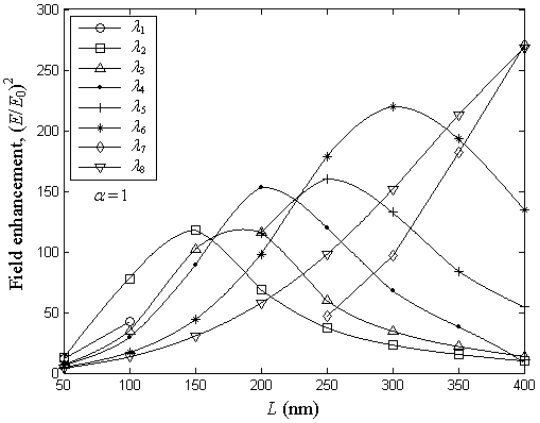

Fig. 10. Variation of $(E/E_0)^2$ at λ_1-λ_8 versus L for the nanoparticles with α=1.

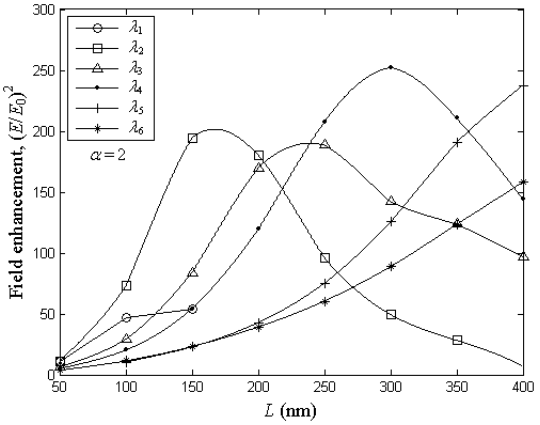

Fig. 11. Variation of $(E/E_0)^2$ at λ_1-λ_6 versus L for the nanoparticles with α=2.

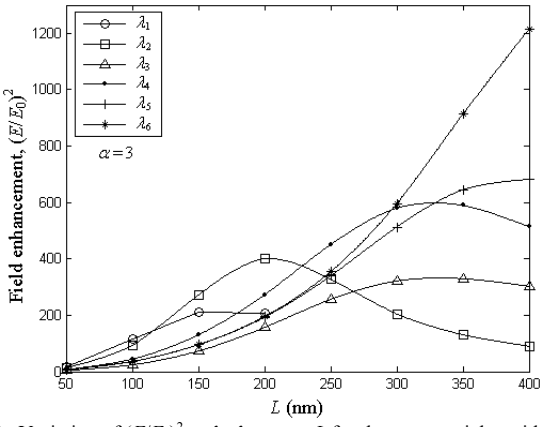

Fig. 12. Variation of $(E/E_0)^2$ at λ_1-λ_6 versus L for the nanoparticles with α=3.

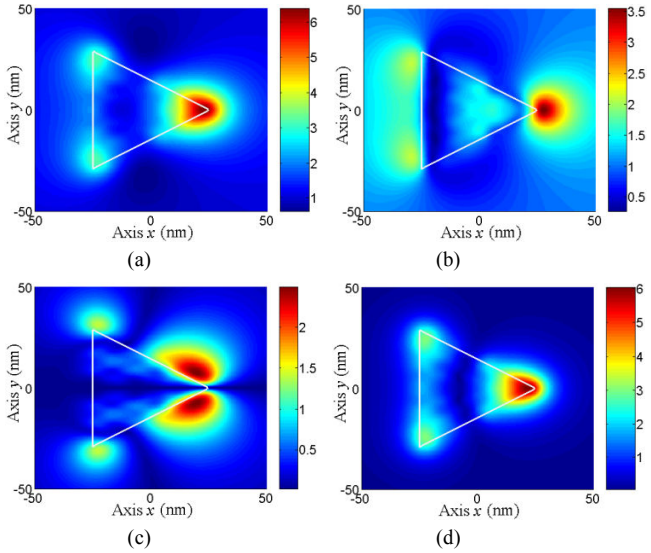

Fig. 13. Field distribution at the plane z=9nm for α=1, L=150nm, λ_2=703nm. (a) E/E_0. (b) E_x/E_0. (c) E_y/E_0. (d) E_z/E_0.

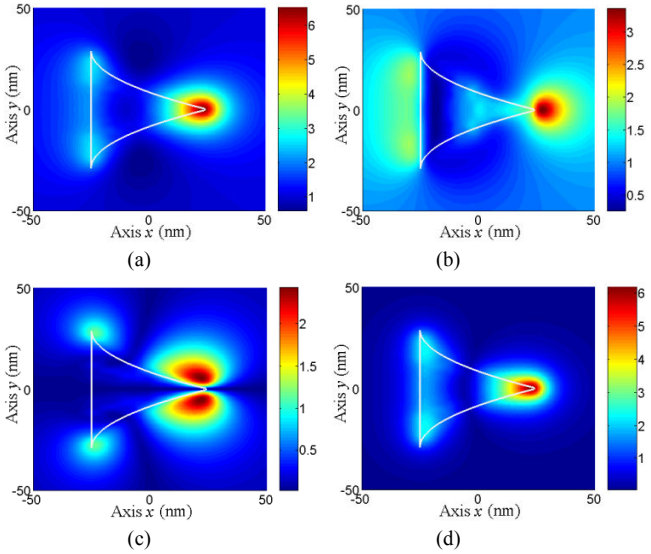

Fig. 14. Field distribution at the plane z=9nm for α=2, L=150nm, λ_2=827nm. (a) E/E_0. (b) E_x/E_0. (c) E_y/E_0. (d) E_z/E_0.

We also observe from these figures that the magnitude of the z electric field component is higher than the others at this plane. This occurs because the normal electric field on the surface's conductor of the particles is larger, and the plane z=9nm is parallel and near the surface's particles. With relation to x component, it is more confined in the region in front of the tips for x>0.5h (Figs. 13b, 14b, 15b, and 16b). The other components in this region are very small. This is due the large concentration of charges in the tips, which produces strong electric fields towards the x direction. This component is important, for example, in applications of nanoantennas, e.g. nanodipoles, for enhancement the spontaneous emission of single molecules within the dipole's gap, because the fields within this gap possess a strong polarization along the axis of the dipole, and the other components are small [8].

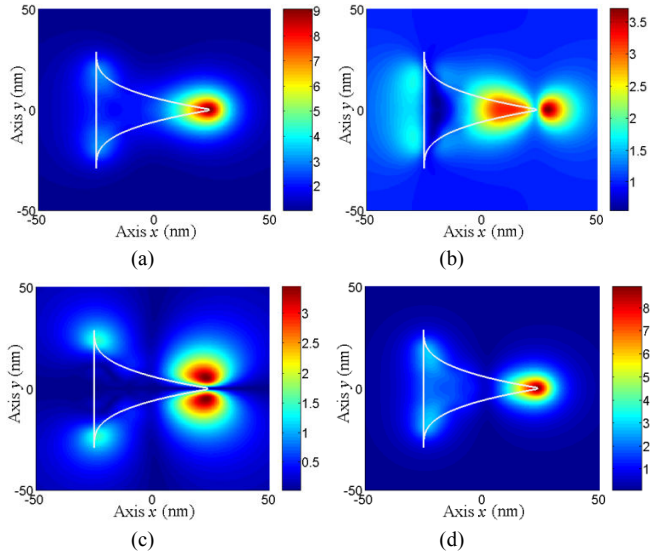

Fig. 15. Field distribution at the plane z=9nm for α=3, L=150nm, λ_1=907nm. (a) E/E_0. (b) E_x/E_0. (c) E_y/E_0. (d) E_z/E_0.

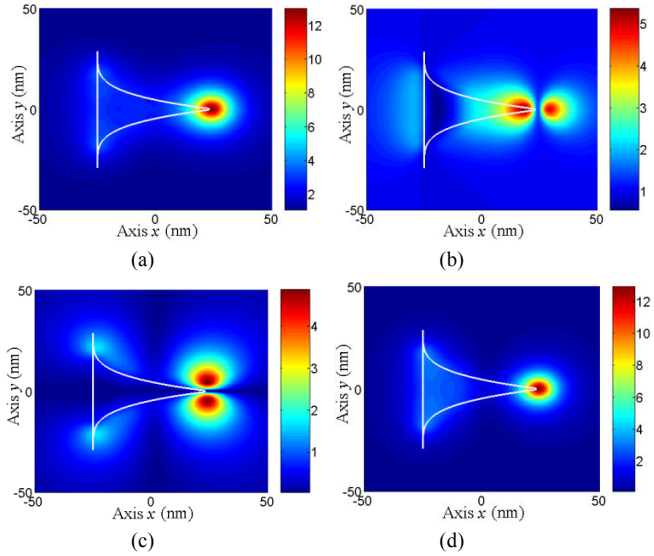

Fig. 16. Field distribution at the plane z=9nm for α=4, L=150nm, λ_1=1096nm. (a) E/E_0. (b) E_x/E_0. (c) E_y/E_0. (d) E_z/E_0.

IV. Conclusions

In this paper, we presented a theoretical analysis of the resonances of modified bowtie nanoparticles with polynomial sides. We observed that the number of resonances of the proposed particles is reduced for larger values of polynomial order in the analyzed wavelength range. For example, the conventional particle presented eight resonances, and the modified one with polynomial order equal to four has two resonances. We also demonstrated that the modified particles have resonant wavelength, near field enhancement and confinement higher than those of the conventional bowtie particle with linear sides. These novel particles can be used to design nanoantennas with better characteristics.

References

[1] L. Novotny, and B. Hecht, *Principles of Nano-Optics*, Cambridge, 2006.
[2] D. W. Pohl, "Near field optics as an antenna problem," *in Proceedings of The Second Asia-Pacific Workshop on Near Field Optics*, pp. 9-21, 1999.
[3] T. H. Taminiau, et al., "Near-Fields driving of a optical monopole antenna," *J. Opt. A: Pure Appl. Opt.*, vol. 9, S315-S321, 2007.
[4] B. Hecht, et al., "Prospects of resonant optical antennas for nano-analysis," *Chimia*, vol. 60, no. 11, pp. 765-769, 2006.
[5] H. Fischer, and O. J. F. Martin, "Engineering the optical response of plasmonic nanoantennas," *Opt. Express*, vol. 16, no. 12, pp. 9144-9154, 2008.
[6] R. Kappeler, et al., "Field computation of optical antennas," *J. Comp. Theor. Nano.*, vol. 4, no. 3, pp. 686-691, 2007.
[7] O. Sqalli, et al., "Gold elliptical nanoantennas as probes for near field optical microscopy," *J. Appl. Phy.*, vol. 92, no. 2, pp. 1078-1083, 2003.
[8] H. Fischer, and O. J. F. Martin, "Engineering the optical response of plasmonic nanoantennas," *Optics Express*, vol. 16, no. 12, pp. 9144-9154, Jun. 2008.
[9] W. Rechberger, et al., "Optical properties of two interacting gold nanoparticles," *Opt. Commu.*, vol. 220, pp. 137-141, 2003.
[10] J. Nelayah, et al., "Mapping surface plasmons on a single metallic nanoparticle," *Nat. Phy.*, vol. 3, pp. 248-353, 2007.
[11] D. E. Livesay, and K. M. Chen, "Electromagnetic fields induced inside arbitrary shaped biological bodies," *IEEE Trans. Micro. Theo. Thec.*, vol. 22, no. 12, pp. 1273-1280, 1974.